Environ Monit Assess (2014) 186:835–843
DOI 10.1007/s10661-013-3420-z

Influence of land use and climate on the load of suspended solids in catchments of Andean rivers

J. Pizarro · P. M. Vergara · J. L. Morales · J. A. Rodríguez · I. Vila

Received: 26 February 2013 / Accepted: 5 September 2013 / Published online: 19 September 2013
© Springer Science+Business Media Dordrecht 2013

Abstract Understanding the interaction between anthropogenic land use and the rainfall pattern can be crucial to predict changes in total suspended solids (TSS) in streams and rivers. We assessed the effects of land use and annual rainfall on the TSS load of 19 southern Chilean catchments. The results indicated that the concentration of TSS increased in catchments with a rainy regime and greater annual precipitation. TSS load also increased as the surface of open areas increased at the catchment scale and decreased with increasing cover of glaciers and perennial snow. However, we did not find support for models with interaction terms between climate and land use. Results suggest that a regional decrease in annual rainfall accompanied by an increase in the altitude of the zero isotherms, as predicted by climate models, should have multiple effects on TSS. In particular, increased TSS load can be expected from a contraction of glaciers and perennial snow areas as well as the intensification of new crops and urban expansion.

Keywords Suspended solids · Land use · Global warming · Chile

Introduction

Total suspended solids (TSS) are basic abiotic components of aquatic ecosystems, influencing food webs and nutrient cycles (Wood and Armitage 1997; Bartley et al. 2012; Odiyo et al. 2012). An increased TSS concentration in freshwater may have detrimental consequences on water quality and lead to increased costs in drinking water treatment (Hutton et al. 2007; Mahmoudi et al. 2010; Ozyonar and Karagozoglu 2012; Chow et al. 2012). TSS in rivers can act as carriers of heavy metals (Horowitz 1995) and persistent organic pollutants (Thomas and Meybeck 1992), whereas high TSS loads can cause strong impacts on the biogeochemical conditions of coastal areas and sea waters (Xu 2002; Hunter and Walton 2008; Hsua and Lin 2010). Therefore, a crucial step in freshwater management is to determine natural and anthropogenic processes that increase TSS concentration.

Intensive anthropogenic activities at the basin scale can increase the sediment load of rivers and lakes through increasing wind erosion (Neff et al. 2008, see also Fox et al. 2012) and runoff erosion (Zhang et al. 2011; Kavian et al. 2011). Vegetation removal, forest fires, intensive agricultural practices, and other anthropogenic activities at the basin scale result in the runoff of soil materials into adjacent streams and rivers (Amiri and Nakane 2006; Zucca et al. 2010; Solaimani et al. 2009; Basso et al. 2012).

J. Pizarro (✉) · J. A. Rodríguez
Departamento de Ingeniería Geográfica, Facultad de Ingeniería, Universidad de Santiago de Chile (Usach), Av. Lib. B. O'Higgins no. 3363, Santiago, Chile
e-mail: jaime.pizarro@usach.cl

P. M. Vergara · J. L. Morales
Departamento de Gestión Agraria, Facultad Tecnológica, Universidad de Santiago de Chile (Usach), Av. Lib. B. O'Higgins no. 3363, Santiago, Chile

I. Vila
Departamento de Ciencias Ecológicas, Facultad de Ciencias, Universidad de Chile, P.O. Box 653, Santiago, Chile

This is of special importance in Andean rivers where natural lithogenic characteristics and mining activities have accelerated natural leaching and weathering. The decline of water quality in Chilean rivers and lakes is a growing concern for environmental policy and land managers (Pizarro et al. 2010a, b). In particular, the replacement of native forest by high water-demanding forest plantations and the intensification of agricultural practices could be attributed to an increase in sediment load in streams and shallow lakes of Chile, as suggested by some previous studies (Cisternas et al. 1999; Pepin et al. 2010). Although intensive land use can increase TSS load in Chilean rivers, natural dynamic processes such as rainfall amounts may also contribute to increase the runoff erosion in river basins (Bathurst et al. 2011; Bonilla and Vidal 2011; Mahmoudi et al. 2010; Kavian et al. 2011). These effects are important as the rainfall regime of central and southern Chilean responds to long-term trends in climate conditions (Quintana and Aceituno 2012). In this study, we used a 23-year database of TSS load in southern Chilean river catchments (Table 1; Fig. 1) to determine if catchments with intensive anthropogenic land use and high amounts of annual rainfall have larger TSS loads. On the basis of these results, and considering future climate scenarios for the region, we discuss possible changes in the sediment load of southern Chilean catchments.

Materials and methods

Study basins

We studied 19 different river catchments of southern Chile (from 33º53′ to 39º50′ S lat., Fig. 2). River catchments were delimited using topographic and hydrological geographic information system (GIS) layers provided by the Ministry of Public Works of Chile. Each basin was associated with its corresponding monitoring sampling station (see below). Soil characteristics of these catchments were homogeneous, as they are of volcanic origin (i.e., Andisols). The studied catchments were located in the Andean mountains (Table 1; Fig. 2). Since rain and snow precipitation can have different effects on sediment runoff (Iida et al. 2012), catchments were classified according to their dominant climate regime by distinguishing between rain and mixed rain–snow basins. Mixed rain–snow basins are characterized by having winter and summer floods, since snow melting occurs during the warm season. Monthly data series of flow were used to characterize the regime of each river.

Explanatory variables

Land use cover was quantified in each catchment using a GIS land use–vegetation database which allowed us to identify polygons representing the main land use activities at the basin scale (Table 2). Land use was considered as a percentage of the total basin area since basins varied widely in their areas. We also measured the mean annual precipitation of each river catchment based on a monthly time series. For this analysis, we developed annual precipitation GIS layers estimating the average amount of water (rain and snow) of the whole study area. Precipitation layers were generated using Kriging interpolation methodology (ArcGIS 9.2) applied to precipitation values drawn from 328 weather stations of the "Dirección General de Aguas" (DGA).

TSS data

We used TSS data from the National River Monitoring Network of the DGA (Table 3). Sampling stations are monitored monthly for TSS and flow data. TSS were manually collected at the sampling stations and filtered using pre-weighed filters, according to the following criteria: at low water levels superficial water samples were collected by filling a bottle until of 75 % of its volume, while at high water levels, the samples were collected from depth-integrated vertical profiles.

Data analysis

We assessed the patterns of TSS concentration (in milligrams per liter) and the slope (in megatons per cubic kilometer) of the double mass curve (DMC) of each catchment. DMCs were estimated by regressing the cumulative annual sediment load on the cumulative annual water discharge (i.e., double mass plots). The slope of such curves represents a measure of the temporal trend of sediment flux relative to that of water discharge and thus they are comparable between basins with different flow levels (Dang et al. 2010). Therefore, these slopes represent an appropriated estimate of the long-term sediment load in our study catchments, where

Table 1 Summary of sampling stations and their associated river catchments

Sampling station	*n*	Regime	Altitude	Flow Mean ± SE	Precipitation Mean ± SE	Land use (%)								
						Native forest	Forest plantation	Agriculture	Open areas	Water bodies	Pasture	Glacier	Urban	Wetlands
A1	201	Rainy–snowy	900	18.7±0.5	1,395.6±95.5	11.38	0.23	0.38	44.64	0.73	35.90	6.71	0.02	0.00
A2	255	Rainy–snowy	900	55.3±0.9	1,395.6±95.5	11.59	0.23	0.38	44.54	0.73	35.82	6.70	0.02	0.00
B1	157	Snowy	6	382.4±11.2	1,410.0±91.4	25.75	0.00	36.81	0.00	1.61	31.67	3.53	0.47	0.15
C1	212	Rainy–snowy	500	94.7±3.4	2,176.9±128.0	46.92	0.00	2.62	27.79	0.38	8.08	14.19	0.02	0.00
C2	151	Rainy–snowy	70	24.1±0.9	1,757.5±99.5	44.39	0.00	29.18	13.28	0.40	6.68	5.38	0.67	0.02
C3	170	Snowy	900	18.6±1.3	2,183.3±118.9	75.99	0.00	3.09	6.20	0.39	3.52	10.55	0.26	0.00
D1	175	Rainy	7	920.3±24.2	1,628.3±815	54.12	0.00	20.88	2.00	2.25	16.37	3.81	0.42	0.15
D2	213	Rainy–snowy	310	391.9±10.4	1,852.5±947	87.22	0.00	0.00	0.00	0.00	12.78	0.00	0.00	0.00
D3	184	Rainy	260	41.3±1.7	2,043.7±106.8	34.21	0.00	2.14	9.74	4.30	33.37	15.48	0.09	0.67
D4	183	Rainy	120	137.5±2.6	1,877.7±97.0	40.27	0.00	3.46	7.93	3.78	30.91	12.92	0.10	0.64
D5	192	Rainy	75	49.1±1.3	1,846.0±94.7	57.46	0.00	18.99	0.47	1.01	15.76	6.16	0.14	0.01
E1	106	Rainy	62	13.9±0.5	1,694.4±75.5	37.33	0.00	56.21	0.05	0.12	5.59	0.00	0.66	0.05
E2	175	Rainy–snowy	420	94.4±2.1	1,560.4±59.8	22.08	0.00	70.46	0.00	0.53	6.33	0.00	0.42	0.18
E3	220	Rainy	23	103.4±3.1	983.3±42.3	23.48	0.00	75.67	0.00	0.37	0.29	0.00	0.00	0.18
E4	213	Rainy–snowy	120	129.0±3.5	2,009.4±92.8	52.36	0.00	18.47	6.17	0.73	18.47	3.80	0.00	0.00
E5	197	Rainy	74	84.7±2.6	1,807.3±70.3	31.24	0.00	57.91	0.28	0.05	9.09	1.12	0.19	0.12
F1	201	Rainy–snowy	204	129.2±2.7	2,052.3±84.6	1.05	0.00	17.27	9.26	6.95	58.37	7.10	0.00	0.00
F2	167	Rainy	81	17.9±1.3	2,098.1±76.5	17.38	0.00	6.64	0.00	0.01	75.59	0.00	0.38	0.00
F3	172	Rainy–snowy	355	107.3±3.1	2,802.3±134.1	64.89	0.00	0.04	6.63	0.58	26.06	1.07	0.04	0.69

Includes sample size (number of TSS records, *n*), climate (regime type and annual mean precipitation in millimeter per year), topography (altitude in meters above sea level), hydrology (annual mean flow in cubic meter per second), and land use characteristics (percentage of land cover). Each sampling station, represented by a particular code, is located in Fig. 1

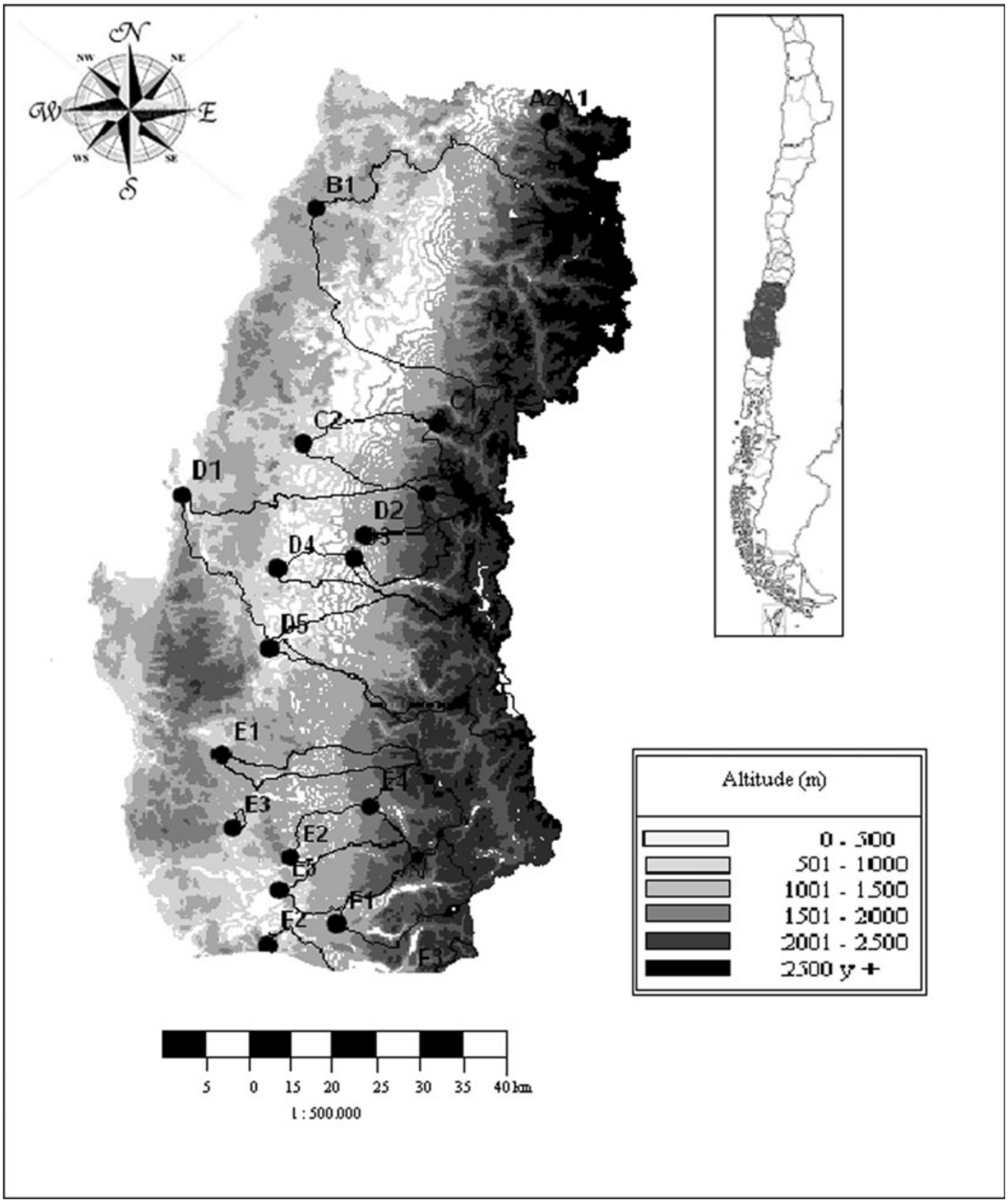

Fig. 1 Map of the 19 river catchments studied in the southern Chilean region (sampling stations, each one represented by a code, are described in Table 1)

sediment load associates positively and linearly with suspended sediment load (Pepin et al. 2010). We used mixed-effects linear models (MLE) to determine the effects of annual precipitation and land use variables on TSS concentration (Venables and Ripley 2002). For these analyses, we used a nested error structure considering the principal basin as a grouping factor and hence controlling for similitude in TSS data from stations belonging to the same principal river (Pizarro et al. 2010a). Additionally, we used a first order autocorrelation structure to control for possible temporal dependence in data. TSS concentration was normalized by log transforming it whereas precipitation was standardized per catchment. Since precipitation and water discharge

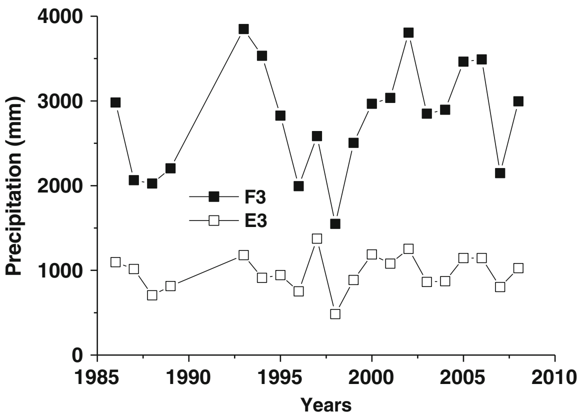

Fig. 2 Annual precipitation amounts of two study catchments. These two catchments differ widely in their precipitation amounts

were correlated ($r>0.64$, $p<0.01$), we used the residuals of a regression of flow on precipitation as a flow estimate corrected by precipitation. Flow was retained in all models because it correlates positively with sediment load (Pepin et al. 2010) whereas basin area was included as an offset variable. We used linear regression analysis for estimating the DMC slope (in megatons per cubic kilometer). Since our interest was focused on comparing annual trends of sediment flux between catchments, we fitted a simple regression line without intercept to each time series. The slopes of such lines were correlated with land use variables and mean annual precipitation. Akaike's Information Criterion (AIC) was used to evaluate the support for competing models including land use, climate, and flow variables (Burnham and Anderson 2002; Table 2). Models were ranked from most to least supported based on ΔAICc (the difference in AICc between the model with the smallest AICc value and the current model). Only models with ΔAICc ≤3 were considered as evidence for supporting hypotheses (Burnham and Anderson 2002).

Table 2 Summary of land use variables which were used as explanatory variables in TSS models

Variable code	Description
Forest plantation	Exotic plantation forest cover
Native forest	Native forest cover, mostly *Pinus radiata*
Agriculture	Commercial crop cover, including wheat and barley
Open areas	Areas without vegetation
Water bodies	Cover of lakes and reservoirs
Pasture	Livestock pasture cover
Glacier	Perennial snow and ice cover in mountain areas
Urban	Urban areas, including cities, towns and conurbations
Wetlands	Wetland cover

Table 3 Means and their standard errors for TSS concentration, mass flow, and the slope of double mass curves of 19 different river catchments studied (see Fig. 1)

Sampling station	TSS concentration mean ± SE	Double mass curve slope ± SE
A1	58.5±5.9	0.080±0.0025
A2	112.8±5.3	0.132±0.0021
B1	26.8±1.3	0.027±0.0003
C1	26.5±3.3	0.056±0.0025
C2	22.6±1.1	0.026±0.0005
C3	7.2±0.4	0.006±0.0001
D1	49.6±2.3	0.058±0.0021
D2	16.8±0.9	0.019±0.0003
D3	10.2±0.4	0.013±0.0001
D4	43.4±1.9	0.046±0.0009
D5	16.6±0.4	0.018±0.0003
E1	24.4±0.8	0.025±0.0009
E2	19.8±0.8	0.022±0.0004
E3	12.0±0.6	0.015±0.0004
E4	21.8±1.8	0.033±0.0010
E5	24±2.7	0.037±0.0002
F1	13.2±2.2	0.021±0.0002
F2	8.7±0.3	0.010±0.0002
F3	19±1.4	0.024±0.0001

Table 4 Best regression models accounting for TSS concentration of river catchments in southern Chile

Model variables	AIC	LogLik	ΔAIC	*w*
TSS concentration				
Precipitation + urban +flow	900.3	−443.1	0.00	0.41
Precipitation + regime + flow + open areas + glacier	901.1	−440.5	0.75	0.28
Flow + precipitation + urban + forest plantation + agriculture	901.7	−441.9	1.41	0.20
Flow + precipitation + urban + open areas	902.8	−443.4	2.53	0.11

Models are ranked by their differences in AIC (ΔAIC) and Akaike weights (*w*)

Table 5 Estimates of regression coefficients, SE, and p values of the best supported models accounting for TSS concentration of 19 different catchments in southern Chile (Table 3)

Variable	Value	Std. error	t Value	p Value
Flow	0.38	0.06	6.20	0.000
Precipitation	0.22	0.05	4.88	0.000
Urban	1.15	0.29	3.95	0.000
Forest plantation	7.48	3.00	2.49	0.067
Regime	−1.57	0.30	−5.27	0.000
Open areas	0.10	0.03	3.74	0.000
Glacier	−0.23	0.05	−5.03	0.000
Agriculture	0.01	0.01	−1.53	0.127

Results

TSS load

TSS varied widely among catchments, with an annual mean of TSS concentration per basin ranging from 7.2 to 112.8 mg L^{-1} whereas the range of median values was 6.8–129.6 (Table 3). MLEs indicated that TSS concentration was dependent on precipitation, land use, and flow (Table 4). Four different models were supported by AIC during the model selection process (ΔAIC <3). The best model included the effects of flow, precipitation, and urban areas (Table 4). The Akaike weight of the best MLE model (w=0.41) indi-

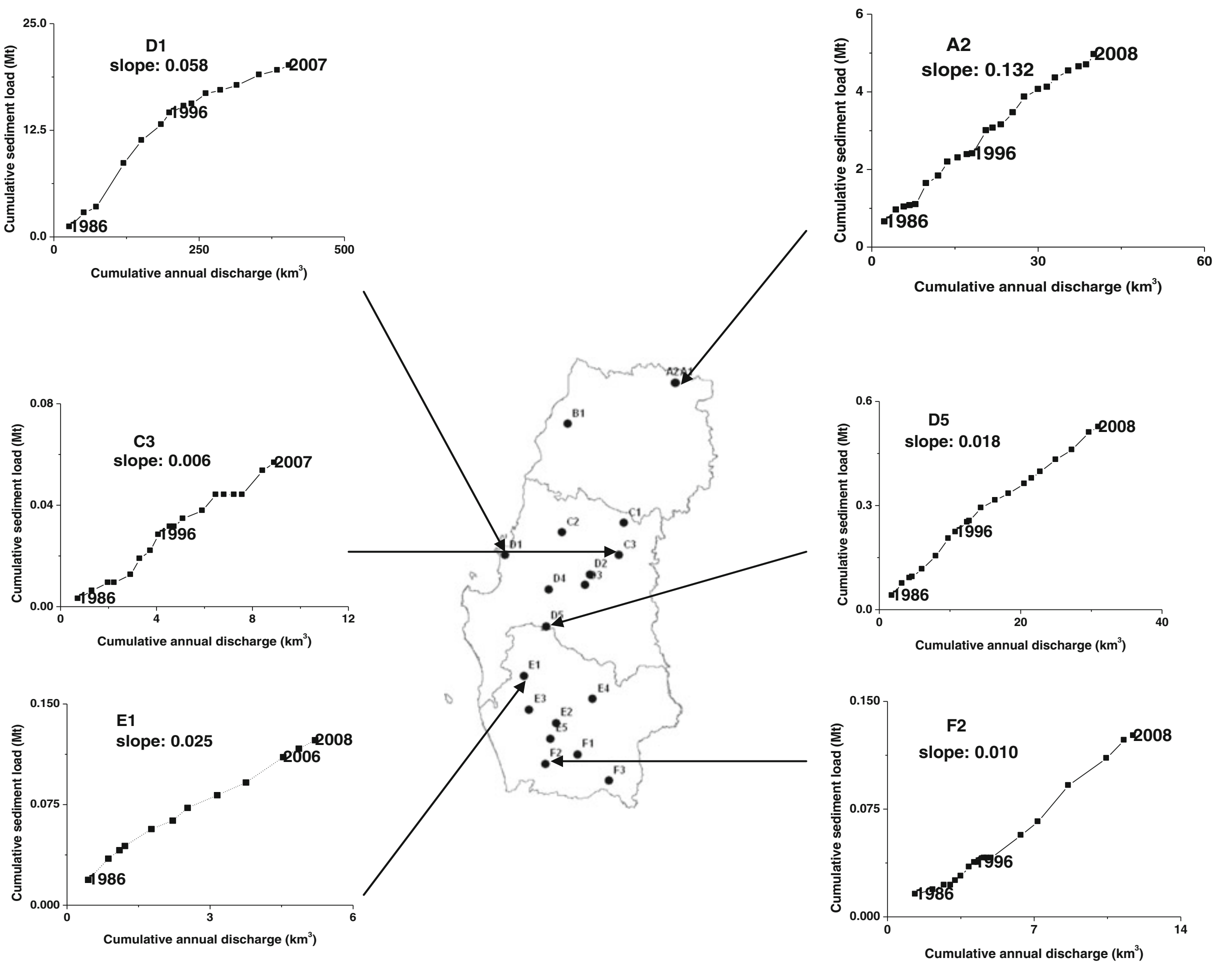

Fig. 3 Double mass plots of six different catchments (see Fig. 1 for code). The slope of linear regressions fitted to the data (DMC) was used as an estimate of the temporal trends in sediment load

cated that this model is only 1.46, 2.03, and 3.54 more likely than the second, third, and fourth best models, respectively, which included the additional effects of climate regime, open areas, glaciers, forest plantations, and agriculture (Table 4). We did not find support for models with interaction terms between climate and land use.

Flow and precipitation had a positive effect on TSS concentration per catchment, while mixed rainy–snowy basins had larger TSS concentrations than rainy basins (Table 5). Catchments with a larger proportion of urban and open areas contributed with more suspended sediments, while forest plantation areas had a marginal effect on TSS concentration ($0.10>p>0.05$; Table 5). Glacier areas per catchment affected TSS concentration negatively (Table 5).

Temporal trends

DMC slopes ranged between 0.006 to 0.132 Mt km^{-3}, with a mean of 0.035±0.007 Mt km^{-3} (Table 3; Fig. 3). The only explanatory variable associated with the DMC slope was the fraction of the total catchment area without vegetation cover (i.e., open areas; r=0.82, p<0.001, n=19; Fig. 4). The other study variables (Table 2) showed weak associations with DMP slope (r<0.24, p>0.450, n=19).

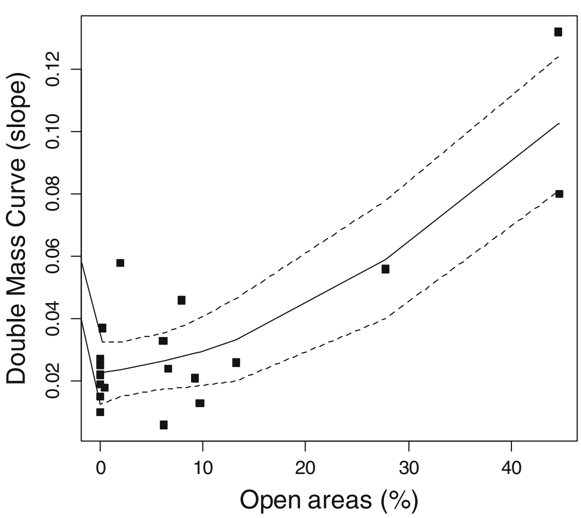

Fig. 4 Scatter plot with the slopes of DMCs versus the percentage of open areas in the 19 study catchments. *Continuous and dashed lines* represent a smooth (cubic spline) function and its confidence intervals, respectively

Discussion

Factors explaining TSS load

The study basin catchments presented mean annual values of TSS concentration that are relatively lower than those reported in other rivers around the world. Indeed, southern Chilean catchments hold sediment load values well below those reported in other Andean river catchments (Restrepo and Syvitski 2006; Laraque et al. 2009). Our results showed that years with more precipitation are associated with larger amounts of mass flow and TSS concentration. However, as shown by MLEs, the type of precipitation (i.e., climate regime) contributed significantly to explain the dynamics of suspended sediment load. It is probable that the soils of catchments dominated by snow precipitation are less exposed to erosion than those exposed to rain (Iida et al. 2012). Furthermore, the accumulation of snow over the ground can eventually reduce rain erosion by acting as a natural protection cover (Wade and Kirkbride 1998). These findings contrast with conclusions of Pepin et al.'s (2010) study which found a positive effect of glacier cover on mean suspended sediment load. However, such study also considered southern Patagonian basins which have a runoff regime influenced mainly by glaciers.

TSS load can become important to the extent that soils are more exposed to rain erosion due to the loss of natural vegetation for agriculture and other economic activities (Milliman 2001 and references therein). Particularly the proportion of urban and open areas contributed positively to increase TSS concentration and mass flow in southern Chilean catchments. It is probable that TSS is increased by the contribution of residual waters from domestic, agro-industrial activities, and urban areas (Zhao et al. 2010; Chow et al. 2012). In open areas (i.e., areas without vegetation cover), the soil surface is largely exposed to the detrimental erosive effects of rainfall (Solaimani et al. 2009; Mahmoudi et al. 2010; Kavian et al. 2011). Furthermore, analysis of the slopes of DMPs indicated that sediment load tends to increase over time in those catchments containing a greater proportion of open areas (e.g., see Fig. 4). Thus, sediment load can become critical in the mid- and long-term to the extent that catchments suffer extensive and intensive soil denudation.

Current climate predictions indicate that total rainfall amounts will decrease about 40 % in the southern Chile region in the next decades, especially over Andean uplands (Boulanger et al. 2007). However, snow will tend to decrease due to the increased altitude of the zero isotherms (Boulanger et al. 2007). As an immediate consequence of such regional climate change, the surfaces covered by glaciers and perennial snows located over mountain areas should decline steeply (Casassa et al. 2007). Thus, a switch in the climate regime from snow to rain precipitation should produce an increase in sediment runoff and erosion (e.g., see Iida et al. 2012). A contraction of glaciers and perennial snow areas in the short term would leave land surfaces previously covered by ice or snow exposed to the erosive effects of wind and rain. This effect can last years (or perhaps a few decades) until the native vegetation gets to colonize those areas. Open areas also can increase in mountain Andean catchments due to improved climate conditions for certain types of crops which previously, it was not possible to cultivate, such as vineyard and peaches (e.g., Garcia-Ruiz 2010). Furthermore, a direct increase in TSS can also result from the expansion of urban areas as a consequence of human population growth in marginal mountain zones. Therefore, on the basis of the latter predictions the declination in TSS load due to a reduction in regional rainfall could be offset by increased TSS load due to interactions between climate warming and land use.

Acknowledgments The authors would like to thank Dirección de Obras Hidráulicas and Dirección General de Aguas for supplying the databases. This study was supported by DICYT 090912PK.

References

Amiri, B. J., & Nakane, K. (2006). Modeling the relationship between land cover and river water quality in the Yamaguchi prefecture of Japan. *Journal of Ecology and Field Biology, 29*, 343–352.

Bartley, R., Speirs, W. J., Ellis, T. W., & Waters, D. K. (2012). A review of sediment and nutrient concentration data from Australia for use in catchment water quality models. *Marine Pollution Bulletin, 65*, 101–116.

Basso, B., De Simone, L., Cammarano, D., Martin, E. C., Margiotta, S., Grace, P. R., et al. (2012). Evaluating responses to land degradation mitigation measures in Southern Italy. *International Journal of Environmental Research, 6*, 367–380.

Bathurst, J. C., Iroumé, A., Cisneros, F., Fallas, J., Iturraspe, R., Gaviño Novillo, M., et al. (2011). Forest impact on floods due to extreme rainfall and snowmelt in four Latin American environments I: field data analysis. *Journal of Hydrology, 400*, 281–290.

Bonilla, C. A., & Vidal, K. L. (2011). Rainfall erosivity in Central Chile. *Journal of Hydrology, 410*, 126–133.

Boulanger, J. P., Martínez, F., & Segura, E. C. (2007). Projection of future climate change conditions using IPCC simulations, neural networks and Bayesian statistics. Part 2: precipitation mean state and seasonal cycle in South America. *Climate Dynamics, 28*, 255–271.

Burnham, K. P., & Anderson, D. R. (2002). *Model selection and inference*. New York: Springer Verlag.

Casassa, G., Haeberli, W., Jones, G., Kaser, G., Ribsteine, P., Rivera, A., et al. (2007). Current status of Andean glaciers. *Global and Planetary Change, 59*, 1–9.

Chow, M. F., Yusop, Z., & Toriman, M. E. (2012). Modeling runoff quantity and quality in tropical urban catchments using Storm Water Management Model. *International Journal of Environmental Science and Technology, 9*, 737–748.

Cisternas, M., Martínez, P., Oyarzun, C., & Debels, P. (1999). Caracterización del proceso de reemplazo de vegetación nativa por plantaciones forestales en una cuenca lacustre de la Cordillera de Nahuelbuta, VIII Región, Chile. *Revista Chilena de Historia Natural, 72*, 661–676.

Dang, T. H., Coynel, A., Orange, D., Blanc, G., Etcheber, H., & Le, L. A. (2010). Long-term monitoring (1960–2008) of the river-sediment transport in the Red River Watershed (Vietnam): temporal variability and dam-reservoir impact. *Science of the Total Environment, 408*, 4654–4664.

Fox, T. A., Barchyn, T. E., & Hugenholtz, C. H. (2012). Successes of soil conservation in the Canadian Prairies highlighted by a historical decline in blowing dust. *Environmental Research Letters*. doi:10.1088/1748-9326/7/1/014008.

Garcia-Ruiz, J. M. (2010). The effects of land uses on soil erosion in Spain: a review. *Catena, 81*, 1–11.

Horowitz, A. J. (1995). *The use of suspended sediment and associated trace elements in water quality studies. International Association of Hydrological Sciences Special Publication No. 4*. Wallingford: IAHS Press.

Hsua, S. C., & Lin, F. J. (2010). Elemental characteristics of surface suspended particulates of the Changjiang estuary during the 1998 flood. *Journal of Marine Systems, 81*, 323–334.

Hunter, H. M., & Walton, R. S. (2008). Land-use effects on fluxes of suspended sediment, nitrogen and phosphorus from a river catchment of the Great Barrier Reef, Australia. *Journal of Hydrology, 356*, 131–146.

Hutton, G., Haller, L., & Bartram, J. (2007). Global cost-benefit analysis of water supply and sanitation interventions. *Journal of Water and Health, 5*, 481–502.

Iida, T., Kajihara, A., Okubo, H., & Okajima, K. (2012). Effect of seasonal snow cover on suspended sediment runoff in a mountainous catchment. *Journal of Hydrology, 428–429*, 116–128.

Kavian, A., Fathollah, N. Y., Habibnejad, M., Soleimani, K., Kavian, A., Fathollah, et al. (2011). Modeling seasonal rainfall erosivity on a regional scale: a case study from Northeastern Iran. *International Journal of Environmental Research, 5*, 939–950.

Laraque, A., Bernal, C., Bourrel, L., Darrozes, J., Christophoul, F., Armijos, E., et al. (2009). Sediment budget of the Napo river, Amazon basin, Ecuador and Peru. *Hydrological Processes, 23*, 3509–3524.

Mahmoudi, B., Bakhtiari, F., Hamidifar, M., Kar, A. D., Mahmoudi, B., Bakhtiari, F., et al. (2010). Effects of land use change and erosion on physical and chemical properties of water (Karkhe watershed). *International Journal of Environmental Research, 4*, 217–228.

Milliman, J. D. (2001). Delivery and fate of fluvial water and sediment to the sea: a marine geologist's view of European rivers. *Scientia Marina, 65*, 121–131.

Neff, J. C., Ballantyne, A. P., Farmer, G. L., Mahowald, N. M., Conroy, J. L., Landry, C. C., et al. (2008). Increasing Aeolian dust deposition in the western United States linked to human activity. *Nature Geoscience, 1*, 189–195.

Odiyo, J. O., Chimuka, L., Mamali, M. A., & Fatoki, O. S. (2012). Trophic status of Vondo and Albasini Dams; impacts on aquatic ecosystems and drinking water model. *International Journal of Environmental Science and Technology, 9*, 203–218.

Ozyonar, F., & Karagozoglu, B. (2012). Systematic assessment of electrocoagulation for the treatment of marble processing wastewater. *International journal of Environmental Science and Technology, 9*, 637–646.

Pepin, E., Carretier, S., Guyot, J. L., & Escobar, F. (2010). Specific suspended sediment yields of the Andean rivers of Chile and their relationship to climate, slope and vegetation. *Hydrological Sciences Journal, 55*, 1190–1205.

Pizarro, J., Vergara, P. M., Rodríguez, J., & Valenzuela, A. M. (2010a). Heavy metal in northern Chilean rivers: spatial variation and temporal trends. *Journal of Hazardous Materials, 181*, 747–754.

Pizarro, J., Vergara, P. M., Rodríguez, J. A., Sanhueza, P. A., & Castro, S. A. (2010b). Nutrients dynamics in the main river basins of the centre-southern region of Chile. *Journal of Hazardous Materials, 175*, 608–613.

Quintana, J. M., & Aceituno, P. (2012). Changes in the rainfall regime along the extratropical west coast of South America (Chile): 30–43 degrees S. *Atmosfera, 25*, 1–22.

Restrepo, J. D., & Syvitski, J. P. M. (2006). Assessing the effect of natural controls and land use change on sediment yield in a major Andean river: the Magdalena drainage basin, Colombia. *Ambio, 35*, 65–74.

Solaimani, K., Modallaldoust, S., & Lotfi, S. (2009). Investigation of land use changes on soil erosion process using geographical information system. *International Journal of Environmental Science and Technology, 6*, 415–424.

Thomas, R., & Meybeck, M. (1992). In D. Chapman (Ed.), *The use of particulate material. Water quality assessments* (pp. 121–170). London: Chapman and Hall.

Venebkes, W. N., & Ripley, B. D. (2002). *Modern applied statistics with S* (4th ed.). New York: Springer.

Wade, R. J., & Kirkbride, M. P. (1998). Snowmelt-generated runoff and soil erosion in Fife, Scotland. *Earth Surface Processes and Landforms, 23*, 123–132.

Wood, P. J., & Armitage, P. D. (1997). Biological effects of fine sediment in the lotic environment. *Environmental Management, 21*, 203–217.

Xu, J. (2002). Implication of relationships among suspended sediment size, water discharge and suspended sediment concentration: the Yellow River basin, China. *Catena, 49*, 289–307.

Zhang, W. G., An, S. Q., Xu, Z., Cui, J., & Xu, Q. (2011). The impact of vegetation and soil on runoff regulation in headwater streams on the east Qinghai–Tibet Plateau, China. *Catena, 87*, 182–189.

Zhao, H., Li, X., Wang, X., & Tian, D. (2010). Grain size distribution of road-deposited sediment and its contribution to heavy metal pollution in urban runoff in Beijing, China. *Journal of Hazardous Materials, 183*, 203–210.

Zucca, C., Canu, A., & Previtali, F. (2010). Soil degradation by land use change in an agropastoral area in Sardinia (Italy). *Catena, 83*, 46–54.